ChemComm

Direct cation exchange of surface ligand capped upconversion nanocrystals to produce strong luminescence

Journal:	*ChemComm*
Manuscript ID	CC-COM-06-2018-004924.R1
Article Type:	Communication

Journal Name

COMMUNICATION

Direct cation exchange of surface ligand capped upconversion nanocrystals to produce strong luminescence

Received 00th January 20xx,
Accepted 00th January 20xx

DOI: 10.1039/x0xx00000x

www.rsc.org/

Ming Guan,[a b] Zhiguang Zhou,[a] Lefu Mei,[b] Hong Zheng,[b] Wei Ren,[a] Li Wang,[c] Yi Du,[c] Dayong Jin,[a] and Jiajia Zhou *[a]

We develop a facile and rapid cation exchange method for upconversion nanocrystals (UCNCs) without removing surface ligands. It avoids the tedious pretreatment of as-synthesized UCNCs, and the luminescent intensities of nanocrystals after Tb^{3+} exchange using new method is much stronger than the nanocrystals using conventional cation exchange in water.

Since the new era of nanotechnology in 1960[1], controlled synthesis has created diverse artificial nanomaterials, including quantum dots[2-5], metal nanoparticles[6, 7], defects/elements doped nanoparticles[8-10], and 2D nanomaterials[11, 12]. Most of them show colourful fluorescence for light-based functionality beyond the size/morphology advantages, enabling their enormous application potentials in life science, display, energy harvest, and quantum engineering[13-19]. To enrich the fluorescence colour, nano semiconductors rely on the tuning of bandgap[20], while the doped nano-insulators require elaborate control of the dopants[21]. Repeated synthesis is able to regulate these compositional arrangements but showing resource- and time-consuming shortages. Alternatively, cation exchange allows high-throughput production of multicolour emitting nanoparticles while preserving the original size, morphology, and crystal phase of the nanoparticles. As a facile method, simplified procedure that suitable for the as-synthesized nanoparticles is the key attractiveness to make the cation exchange be extensively adopted.

Here we report a novel cation exchange method for as-synthesized rare-earth doped upconversion nanocrystals (UCNCs), which is emerging as a promising light carrier in different fields[22-28]. Our method can directly exchange the cation ions when the surface of the as-synthesized nanocrystals is capped with ligands. As is well known that wet-chemical route growth of UCNCs produces hydrophobic nanocrystals with monodispersity and stable fluorescence in non-polar solvents because of the surface ligands, e.g., oleic acid. Under the premise of retaining surface ligands, we are able to complete cation exchange within seconds by simply dripping the cation contained solution into the nanocrystals colloid. Compared to conventional cation exchange of UCNCs in water (WACE)[29, 30], our organic solvent allows cation exchange (OSCE) avoiding the tedious pretreatment of as-synthesized UCNCs by removing surface ligands using hydrochloric acid that may damage the peripheral lattices[31, 32]. Furthermore, the coverage of surface ligands helps the nanocrystals to defend against aggregation and degradation that have been observed in water circumstance[32-36].

As illustrated in Figure 1a, we choose solvent X to dissolve rare-earth salts, forming rare-earth cations in solution, while use

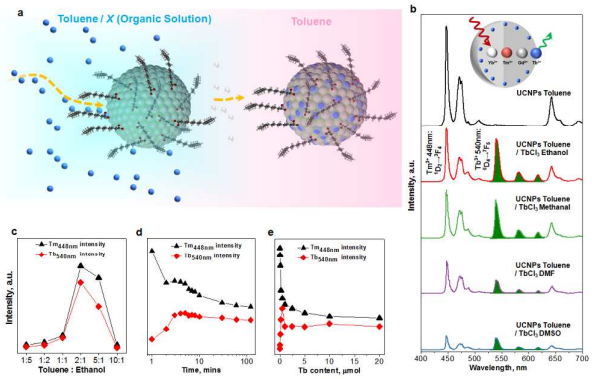

Fig. 1 (a) Schematic illustration of the OSCE (organic solvent allowed cation exchange) procedure. (b) Nanostructure of core-only $NaGdF_4$:Yb^{3+}/Tm^{3+} UCNCs for OSCE, and UC emission spectra of the UCNCs before and after exchange in Toluene/Ethanol, Toluene/Methanol, Toluene/DMF, Toluene/DMSO respectively. (c-e) Emission intensity as a function of toluene/ethanol ratio, exchange time, and Tb^{3+} concentration respectively. All the emission spectra were recorded under the irradiation of a 980 nm laser with power density of 500 mW cm^{-2}.

[a] Institute for Biomedical Materials and Devices, School of Mathematical and Physical Sciences, Faculty of Science, University of Technology, Sydney, NSW 2007, Australia.
[b] School of Materials Science and Technology, Beijing Key Laboratory of Materials Utilization of Nonmetallic Minerals and Solid Wastes, National Laboratory of Mineral Materials, China University of Geosciences, Beijing100083, China.
[c] Institute for Superconducting and Electronic Materials (ISEM), Australian Institute for Innovative Materials (AIIM), University of Wollongong, Wollongong, NSW 2500, Australia.
† Email: Jiajia.Zhou@uts.edu.au

Electronic Supplementary Information (ESI) available: [details of any supplementary information available should be included here]. See DOI: 10.1039/x0xx00000x

toluene to disperse oleic acid capped $NaGdF_4$ UCNCs. Typically, solvent X dissolves $TbCl_3$, and toluene disperses the as-synthesized UCNCs, followed by cation exchange reaction through mixing these two kinds of solutions in appropriate volume ratio at room temperature. Tb^{3+} ions partially replace the rare-earth sites in the crystal structure of $NaGdF_4$:Tm^{3+},Yb^{3+}, forming new $NaGdF_4$:Tm^{3+},Yb^{3+},Tb^{3+} composition. This tridoped system produces Tb^{3+} upconverted emission by capturing the energy populated at the excited states of Tm^{3+} ($^1I_6$) through Yb^{3+} sensitization and Gd^{3+} bridge-like energy migration upon 980 nm laser excitation (Figure S1)[37]. The characteristic emission peaks from Tb^{3+} at 488, 540, 582 and 618 nm (green segments highlighted in Figure 1b) indicate the successful entering of Tb^{3+} in the $NaGdF_4$ crystal sites.

We first prove that the OSCE method is applicable to different solvent X, for example, Methanol, Ethanol, Dimethyl Formamide (DMF), Dimethylsulfoxide (DMSO) (listed by order of increasing polarity indexes of 5.1, 5.2, 6.4, and 7.2, respectively). Tb^{3+} emissions appear in all the mixed solutions of Toluene/Ethanol, Toluene/Methanol, Toluene/DMF, and Toluene/DMSO, indicating that once UCNCs and free ions meet in organic solvent, cation exchange takes place. However, increased polarity of solvent X leads to decreased UC emission intensities due to the weaker intersolubility with non-polar solvent Toluene. Taking Toluene/Ethanol supported OSCE as an example for systematic study, the best volume ratio of toluene and ethanol is 2:1 (Figure 1c), and the exchange happens within 5 seconds while the balance time for exchange 0.5 μM Tb^{3+} is 4 mins (Figure 1d). The emission intensity of Tb^{3+} (monitored at 540 nm) is enhanced by slightly increasing the concentration of the exchange ions, and the optimal concentration of Tb^{3+} in mixed solvents is found to be 0.5 μM (Figure 1e). At the same time, the UC intensity of Tm^{3+} (monitored at 448 nm) deceases monotonically due to the population

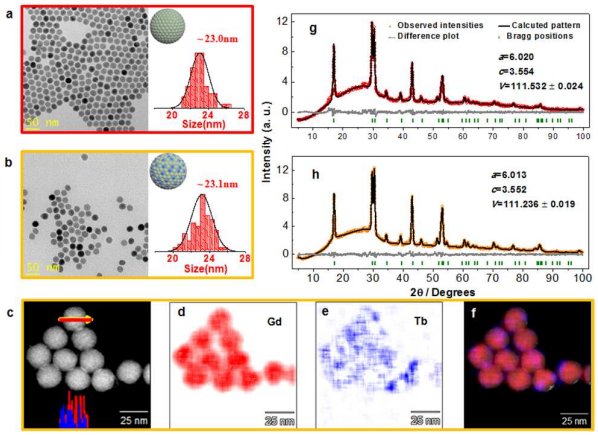

Fig. 2 (a-b) TEM images and size distributions of $NaGdF_4$:Yb^{3+},Tm^{3+} nanocrystals before and after OSCE (by 0.5 μM Tb^{3+}). (c-f) HRTEM and EELS images of $NaGdF_4$:Yb^{3+},Tm^{3+} after OSCE, note that elemental maps of Gd and Tb ions (d-f) reveal that Tb penetrated into the out layer of $NaGdF_4$:Yb^{3+},Tm^{3+} UCNCs. (g-h) XRD patterns and calculated cell parameters and volumes of $NaGdF_4$:Yb^{3+},Tm^{3+} before and after OSCE.

redistribution among excited states when extra Tb^{3+} ions appear in the nanocrystal, opening a new energy pathway from Tm^{3+}:$^1I_6$ to Tb^{3+}: $^5D_4$ through Gd^{3+}: $^6P_{7/2}$ state[21, 38]. At 0.5 μM Tb^{3+} concentration exchange condition, the integrated UC emission intensities area of $NaGdF_4$: Tm^{3+}/Yb^{3+}/Tb^{3+} is about 87.6% of $NaGdF_4$: Tm^{3+}/Yb^{3+} UCNCs template (Figure S2). This OSCE method is also applicable to other rare-earth precursor salts, e.g., rare-earth acetate (Figure S3), as well as the other exchange ions, e.g., Eu^{3+} (Figure S4).

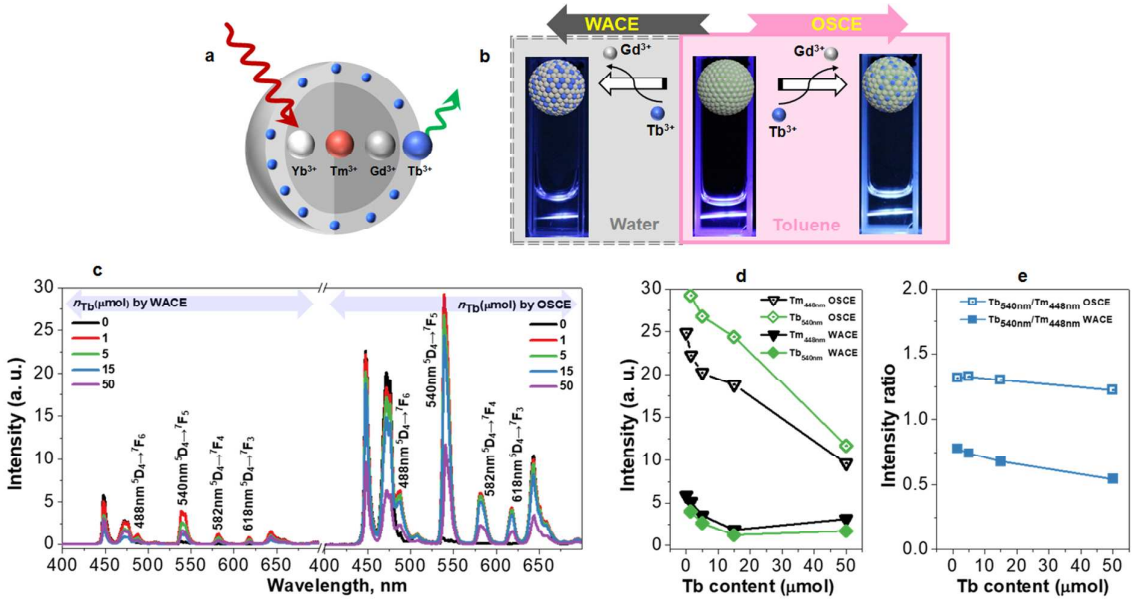

Fig. 3 (a) Nanostructure of core-shell $NaGdF_4$:Yb^{3+},Tm^{3+}@$NaGdF_4$ UCNCs for cation exchange. (b) Luminescent photos of UCNCs by WACE, initial UCNCs template, UCNCs by OSCE under the irradiation of a 980 nm laser. (c) Upconversion emission spectra after cation exchanging through WACE and OSCE respectively (5 different kinds of Tb^{3+} content). The concentrations of all the samples are 1 mg mL^{-1}. (d) Intensities of Tm^{3+} and Tb^{3+} emissions as a function of Tb^{3+} content. (e) Intensity ratio of Tb^{3+}/Tm^{3+} emissions as a function of Tb^{3+} content. All spectra were recorded under 980 nm excitation with power density of 500 mW cm^{-2}.

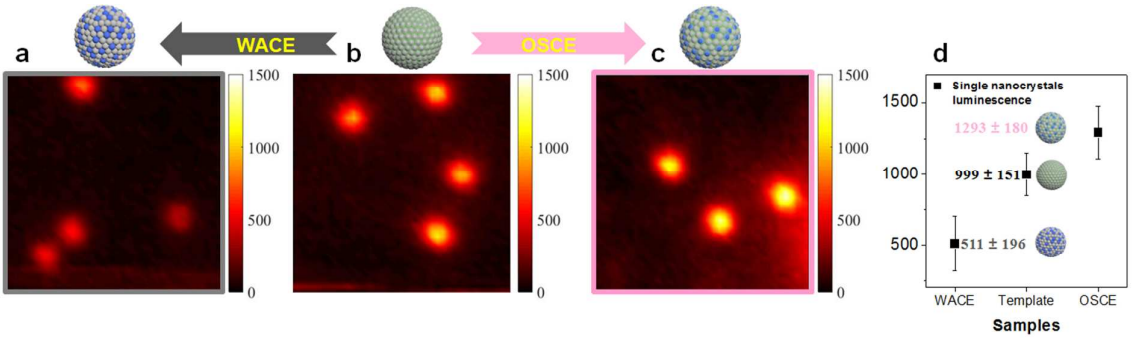

Fig. 4 Confocal scanning images and the averaged brightness of core-shell $NaGdF_4$:Yb^{3+},Tm^{3+}@$NaGdF_4$ single nanocrystals. (a and c) Confocal images of UCNCs by WACE, initial UCNCs template, UCNCs by OSCE respectively (under 1 μM Tb^{3+} exchange). (d) Brightness statistics of the single UCNCs corresponding to a–c. All the optical images were recorded with an 842 nm short pass filter under the irradiation of a 980 nm single mode laser (30 MW cm^{-2}).

To confirm the entrance of exchange ions in the lattice, we perform structural analysis of the nanocrystals. Transmission electron microscopy (TEM) images reveal the particle size and morphology of UCNCs before and after OSCE under 0.5 μM Tb^{3+} ions. Before cation exchange, the size of initial $NaGdF_4$:Yb^{3+},Tm^{3+} UCNCs template is about 23 nm (Figure 2a). After cation exchange in Toluene/Ethanol under ambient conditions for 10 min, the exchanged particles show no obvious changes in terms of particle size (23.1 nm) and morphology (Figure 2b). We further employ high-resolution transmission electron microscopy (HRTEM) imaging and electron energy loss spectroscopy (EELS) to confirm the existence of Tb^{3+} ions (Figure 2 c-f). Combined with the line profile on a single particle (Figure 2c), we can find that Tb^{3+} ions only appear on the surface while Gd^{3+} ions exist in the centre of particles, indicating the enrichment of Tb^{3+} at the surface of UCNCs. We also use the X-ray diffraction (XRD) and Rietveld refinement to characterize the structure evolution in terms of cell parameters and cell volumes (Figure 2 g-h). Both of the X-ray patterns are in line with the hexagonal cell (Pm-63) with parameters close to starting model of ICSD #51920[39], indicating OSCE did not induce variation in particle phase. In the structure of $NaGdF_4$:Yb^{3+},Tm^{3+} UCNCs, Yb^{3+},Tm^{3+},Gd^{3+} ions occupy the same position and have the ionic radius of 1.042, 1.052, 1.107 Å (9 coordination) respectively[40]. Refinements show the initial UCNCs template has unit cell volume of 111.532 $Å^3$ (Figure 2 g). After OSCE by 0.5 μM Tb^{3+} ions (r= 1.095 Å, 9 coordination), the cell volume of $NaGdF_4$:Yb^{3+},Tm^{3+},Tb^{3+} UCNCs decreases to 111.236 $Å^3$, which implies that the small Tb^{3+} mainly replace larger Gd^{3+} ions in the lattice.

To visualize the advantage of OSCE method in retaining the emission intensity of UCNCs, we compare the colloid luminescent intensity/colour and spectroscopic properties of the exchanged UCNCs to the samples using WACE method (Figure 3). By adopting $NaGdF_4$:Yb^{3+},Tm^{3+}@$NaGdF_4$ core-shell structure UCNCs (~16 nm core, ~23 nm core-shell, Figure S5) as template (Figure 3a), it is clearly shown in the photos that the emission intensity of UCNCs after Tb3 +exchange by OSCE is much stronger than that done by WACE in parallel. (Figure 3b). Moreover, the hybrid emitting light from Tb^{3+} and Tm^{3+} by OSCE method tends to be whiter. The comparison of spectroscopic properties (Figure 3c and 3d) shows much stronger emission peaks obtained from the OSCE method, regardless of the Tb^{3+} concentrations for the cation exchange. Though emission intensities of typical Tm^{3+} (448nm) and Tb^{3+} (540 nm) peaks decrease with the increasing Tb^{3+} concentration from 1 to 50 μM (Figure 3d). By calculating the integrated intensity of typical samples (UCNCs by WACE, initial UCNCs template, UCNCs by OSCE, under 1 μM Tb^{3+}), we find that the intensity of UCNCs shows 1.68-fold enhancement after OSCE, whereas the intensity decreases to 27% of the initial template after WACE (Figure S6). The brightness of colloidal UCNCs after Tb^{3+}- OSCE is about 6.2-fold stronger than that of the UCNCs after Tb^{3+}- WACE. Furthermore, The intensity ratio of Tb^{3+}/Tm^{3+} by OSCE is larger than 1, while the ratio of Tb^{3+}/Tm^{3+} by WACE is less than 1 (Figure 3e), implying the UC emissions of Tb^{3+} ions in the UCNCs by OSCE is more efficient. The higher efficient Tb^{3+} emission via OSCE is probably due to the cation exchange depth and concentration of the Tb^{3+} ions per particle, as well as the decrease of possible crystalline defects and/or anionic ions adsorption under maintained surface property. These could affect the energy transfer efficiency from Tm^{3+} to Tb^{3+} via Gd^{3+}, and the radiative emission efficiency of Tb^{3+}. Similar phenomenon happens when Eu^{3+} ions work as the exchange ions (Figure S7), or the other solvents supported exchange process (e.g., Toluene/DMF in Figure S8).

We use a home-made confocal microscope to quantify the emission intensities of the core-shell nanocrystals after Tb^{3+} exchange through OSCE and WACE at single particle level. To achieve high signal-to-noise ratio under confocal microscope for accurate single nanocrystal analysis, we made large size core-shell $NaGdF_4$:Yb^{3+},Tm^{3+}@$NaGdF_4$ (~37 nm core, ~44 nm core-shell, Figure S9). The average brightness of single core-shell UCNCs after Tb^{3+}-WACE is about 511 photon counts (50ms) after background subtraction, which is half as much as the brightness of initial core-shell UCNCs template (999 photon counts, 50ms) (Figure 4a,b,d). For the core-shell UCNCs after Tb^{3+}-OSCE, the average brightness of single particles (1293 photon counts, 50ms) is about 1.3-fold stronger than the brightness of initial core-shell UCNCs template (Figure 4b,c,d). The brightness of single UCNCs after Tb^{3+}- OSCE is about 2.5-fold stronger than that of the UCNCs after Tb^{3+}- WACE.

Conclusions

In summary, we have developed a rapid and facile cation exchange method for UCNCs without removing surface ligands in organic solvent. We have quantitively compared the UC emission properties of UCNCs that is prepared by OSCE method and conventional WACE method in parallel. The WACE shows significantly quenching effect on the fluorescence intensity of UCNCs, whereas the OSCE provides UCNCs much higher intensity in both colloidal and single particle state. Potentially, the maintained surface property becomes the key to stabilize the UCNPs in organic solvents for further growth of other materials. This facile and rapid OSCE synthesis strategy opens a new way to the synthetic methodology for UCNCs with intense luminescence.

The authors acknowledge the financial support from the Australian Research Council (ARC) Discovery Early Career Researcher Award Scheme (J. Z., DE 180100669), Chancellor's Postdoctoral Fellowship Scheme at the University of Technology Sydney (J. Z.), Future Fellowship Scheme (D.J., FT 130100517), the Major International (Regional) Joint Research Project of NSFC (51720105015), the National Natural Science Foundation of China (61729501), and the China Scholarship Council Scholarships (Ming Guan, No. 201506400025).

Conflicts of interest

There are no conflicts to declare.

Notes and references

1 R. Feynman, *Caltech Eng Sci*, 1960, **23**, 22-36.
2 G. Huang, C. Wang, S. Xu, S. Zong, J. Lu, Z. Wang, C. Lu and Y. Cui, *Adv Mater*, 2017, **29**, 1700095.
3 B. J. Beberwyck, Y. Surendranath and A. P. Alivisatos, *J Phys Chem C*, 2013, **117**, 19759-19770.
4 B. A. Koscher, N. D. Bronstein, J. H. Olshansky, Y. Bekenstein and A. P. Alivisatos, *J Am Chem Soc*, 2016, **138**, 12065-12068.
5 D. Dorokhin, N. Tomczak, M. Han, D. N. Reinhoudt, A. H. Velders and G. J. Vancso, *ACS Nano*, 2009, **3**, 661-667.
6 C. Langlois, P. Benzo, R. Arenal, M. Benoit, J. Nicolai, N. Combe, A. Ponchet and M. J. Casanove, *Nano Lett*, 2015, **15**, 5075-5080.
7 K. D. Gilroy, R. A. Hughes and S. Neretina, *J Am Chem Soc*, 2014, **136**, 15337-15345.
8 Vlasov, II, A. A. Shiryaev, T. Rendler, S. Steinert, S. Y. Lee, D. Antonov, M. Voros, F. Jelezko, A. V. Fisenko, L. F. Semjonova, J. Biskupek, U. Kaiser, O. I. Lebedev, I. Sildos, P. R. Hemmer, V. I. Konov, A. Gali and J. Wrachtrup, *Nat Nanotechnol*, 2014, **9**, 54-58.
9 F. Wang, Y. Han, C. S. Lim, Y. Lu, J. Wang, J. Xu, H. Chen, C. Zhang, M. Hong and X. Liu, *Nature*, 2010, **463**, 1061-1065.
10 D. Liu, X. Xu, Y. Du, X. Qin, Y. Zhang, C. Ma, S. Wen, W. Ren, E. M. Goldys, J. A. Piper, S. Dou, X. Liu and D. Jin, *Nat Commun*, 2016, **7**, 10254.
11 X. J. Wu, J. Chen, C. Tan, Y. Zhu, Y. Han and H. Zhang, *Nat Chem*, 2016, **8**, 470-475.
12 C. Tan and H. Zhang, *J Am Chem Soc*, 2015, **137**, 12162-12174.
13 M. T. Berry and P. S. May, *J Phys Chem A*, 2015, **119**, 9805-9811.
14 Q. Liu, W. Feng and F. Li, *Coord Chem Rev*, 2014, **273**, 100-110.
15 Y. Liu, Y. Lu, X. Yang, X. Zheng, S. Wen, F. Wang, X. Vidal, J. Zhao, D. Liu, Z. Zhou, C. Ma, J. Zhou, J. A. Piper, P. Xi and D. Jin, *Nature*, 2017, **543**, 229-233.
16 T.-H. Kim, K.-S. Cho, E. K. Lee, S. J. Lee, J. Chae, J. W. Kim, D. H. Kim, J.-Y. Kwon, G. Amaratunga, S. Y. Lee, B. L. Choi, Y. Kuk, J. M. Kim and K. Kim, *Nat Photonics*, 2011, **5**, 176-182.
17 F. Meinardi, H. McDaniel, F. Carulli, A. Colombo, K. A. Velizhanin, N. S. Makarov, R. Simonutti, V. I. Klimov and S. Brovelli, *Nat Nanotechnol*, 2015, **10**, 878-885.
18 L. P. McGuinness, Y. Yan, A. Stacey, D. A. Simpson, L. T. Hall, D. Maclaurin, S. Prawer, P. Mulvaney, J. Wrachtrup, F. Caruso, R. E. Scholten and L. C. Hollenberg, *Nat Nanotechnol*, 2011, **6**, 358-363.
19 I. Aharonovich, D. Englund and M. Toth, *Nat Photonics*, 2016, **10**, 631-641.
20 R. E. Bailey and S. Nie, *J Am Chem Soc*, 2003, **125**, 7100 - 7106.
21 F. Wang, R. Deng, J. Wang, Q. Wang, Y. Han, H. Zhu, X. Chen and X. Liu, *Nat Mater*, 2011, **10**, 968-973.
22 H. Suo, F. Hu, X. Zhao, Z. Zhang, T. Li, C. Duan, M. Yin and C. Guo, *J Mater Chem C*, 2017, **5**, 1501-1507.
23 M. Haase and H. Schafer, *Angew Chem Int Ed Engl*, 2011, **50**, 5808-5829.
24 E. M. Chan, G. Han, J. D. Goldberg, D. J. Gargas, A. D. Ostrowski, P. J. Schuck, B. E. Cohen and D. J. Milliron, *Nano Lett*, 2012, **12**, 3839-3845.
25 B. Zhou, B. Shi, D. Jin and X. Liu, *Nat Nanotechnol*, 2015, **10**, 924-936.
26 J. Zhao, D. Jin, E. P. Schartner, Y. Lu, Y. Liu, A. V. Zvyagin, L. Zhang, J. M. Dawes, P. Xi, J. A. Piper, E. M. Goldys and T. M. Monro, *Nat Nanotechnol*, 2013, **8**, 729-734.
27 X. Liu, Y. Wang, X. Li, Z. Yi, R. Deng, L. Liang, X. Xie, D. T. B. Loong, S. Song, D. Fan, A. H. All, H. Zhang, L. Huang and X. Liu, *Nat Commun*, 2017, **8**, 899.
28 J. Zhou, S. Wen, J. Liao, C. Clarke, S. A. Tawfik, W. Ren, C. Mi, F. Wang and D. Jin, *Nat Photonics*, 2018, **12**, 154-158.
29 S. Han, X. Qin, Z. An, Y. Zhu, L. Liang, Y. Han, W. Huang and X. Liu, *Nat Commun*, 2016, **7**, 13059.
30 C. Dong, A. Korinek, B. Blasiak, B. Tomanek and F. C. J. M. van Veggel, *Chem Mater*, 2012, **24**, 1297-1305.
31 D. Liu, X. Xu, F. Wang, J. Zhou, C. Mi, L. Zhang, Y. Lu, C. Ma, E. Goldys, J. Lin and D. Jin, *J Mater Chem C*, 2016, **4**, 9227-9234.
32 S. Lahtinen, A. Lyytikäinen, H. Päkkilä, E. Hömppi, N. Perälä, M. Lastusaari and T. Soukka, *J Phys Chem C*, 2016, **121**, 656-665.
33 O. Plohl, S. Kralj, B. Majaron, E. Frohlich, M. Ponikvar-Svet, D. Makovec and D. Lisjak, *Dalton Trans*, 2017, **46**, 6975-6984.
34 D. Lisjak, O. Plohl, M. Ponikvar-Svet and B. Majaron, *RSC Adv*, 2015, **5**, 27393-27397.
35 O. Plohl, M. Kraft, J. Kovac, B. Belec, M. Ponikvar-Svet, C. Wurth, D. Lisjak and U. Resch-Genger, *Langmuir*, 2017, **33**, 553-560.
36 D. Lisjak, O. Plohl, J. Vidmar, B. Majaron and M. Ponikvar-Svet, *Langmuir*, 2016, **32**, 8222-8229.
37 X. Li, X. Liu, D. Chevrier, X. Qin, X. Xie, S. Song, H. Zhang, P. Zhang and X. Liu, *Angew Chem*, 2015, **127**, 13510–13515.
38 C. Zhang, L. Yang, J. Zhao, B. Liu, M. Y. Han and Z. Zhang, *Angew Chem Int Ed Engl*, 2015, **54**, 11531-11535.
39 A. Grzechnik, P. Bouvier, M. Mezouar, M. D. Mathews, A. K. Tyagi and J. Köhler, *J Solid State Chem*, 2002, **165**, 159-164.
40 R. D. Shannon, *Acta Crystallogr A*, 1976, **32**, 751-767.